Report

Current Biology

Cellular Innovation of the Cyanobacterial Heterocyst by the Adaptive Loss of Plasticity

Highlights

- A novel nitrogen-fixing heterocyst has evolved multiple times in *Fischerella*
- The envelopes of these heterocysts are less permeable than those of ancestral cells
- This is adaptive at high temperature but results in ecological specialization
- Adaptation involved loss of phenotypic plasticity and has a simple genetic basis

Authors

Scott R. Miller, Reid Longley, Patrick R. Hutchins, Thorsten Bauersachs

Correspondence

scott.miller@umontana.edu (S.R.M.), thorsten.bauersachs@ifg.uni-kiel.de (T.B.)

In Brief

Cellular innovation is central to biological diversification, but its mechanisms are poorly understood. Miller et al. show that a structurally novel nitrogen-fixing cell has evolved multiple times during high-temperature adaptation by the cyanobacterium *Fischerella thermalis*. Adaptation involved the loss and refinement of developmental variation.

Miller et al., 2020, Current Biology *30*, 1–7
January 20, 2020
https://doi.org/10.1016/j.cub.2019.11.056

CellPress

Please cite this article in press as: Miller et al., Cellular Innovation of the Cyanobacterial Heterocyst by the Adaptive Loss of Plasticity, Current Biology (2019), https://doi.org/10.1016/j.cub.2019.11.056

Current Biology
Report

CellPress

Cellular Innovation of the Cyanobacterial Heterocyst by the Adaptive Loss of Plasticity

Scott R. Miller,[1,3,*] Reid Longley,[1] Patrick R. Hutchins,[1] and Thorsten Bauersachs[2,*]
[1]Division of Biological Sciences, University of Montana, Missoula, MT 59812, USA
[2]Institute of Geosciences, Department of Organic Geochemistry, Christian-Albrechts-University, 24118 Kiel, Germany
[3]Lead Contact
*Correspondence: scott.miller@umontana.edu (S.R.M.), thorsten.bauersachs@ifg.uni-kiel.de (T.B.)
https://doi.org/10.1016/j.cub.2019.11.056

SUMMARY

Cellular innovation is central to biological diversification, yet its underlying mechanisms remain poorly understood [1]. One potential source of new cellular traits is environmentally induced phenotypic variation, or phenotypic plasticity. The plasticity-first hypothesis [2–4] proposes that natural selection can improve upon an ancestrally plastic phenotype to produce a locally adaptive trait, but the role of plasticity for adaptive evolution is still unclear [5–10]. Here, we show that a structurally novel form of the heterocyst, the specialized nitrogen-fixing cell of the multicellular cyanobacterium *Fischerella thermalis*, has evolved multiple times from ancestrally plastic developmental variation during adaptation to high temperature. Heterocyst glycolipids (HGs) provide an extracellular gas diffusion barrier that protects oxygen-sensitive nitrogenase [11, 12], and cyanobacteria typically exhibit temperature-induced plasticity in HG composition that modulates heterocyst permeability [13, 14]. By contrast, high-temperature specialists of *F. thermalis* constitutively overproduce glycolipid isomers associated with high temperature to levels unattained by plastic strains. This results in a less-permeable heterocyst, which is advantageous at high temperature but deleterious at low temperature for both nitrogen fixation activity and fitness. Our study illustrates how the origin of a novel cellular phenotype by the genetic assimilation and adaptive refinement of a plastic trait can be a source of biological diversity and contribute to ecological specialization.

RESULTS AND DISCUSSION

Convergent Losses of Heterocyst Composition Plasticity during High Temperature Adaptation

Most organisms experience environmental variation during their lifetimes, and many have the capacity to respond to changing conditions by expressing different phenotypes in different environments (i.e., phenotypic plasticity). This ability may improve an individual's fitness across a broader range of conditions than would a fixed phenotype. However, constraints on plasticity may preclude an optimal phenotype-environment match under certain conditions [15–18]. The plasticity-first hypothesis [2–4] proposes that natural selection can refine an ancestrally plastic phenotype into a novel locally adaptive trait that better matches the environment. This may involve the evolution of constitutive expression of the new trait through the loss of environmental sensitivity, i.e., genetic assimilation [19–21]. Genetic assimilation may overcome the potential limits as well as any intrinsic costs of plasticity (e.g., the maintenance of sensory machinery) but may also result in the evolution of ecological specialization through a reduction in niche breadth [15, 22–24].

The plasticity-first hypothesis remains controversial, however, due to long-standing disagreement regarding the role of plasticity for adaptation [2, 5–10]. For example, plasticity may potentially facilitate adaptation by presenting a greater range of phenotypes for selection to act on, which may be of particular relevance for diversification in extreme or stressful environments [2, 25, 26]. Alternatively, it may instead limit an adaptive response by buffering individuals from environmental change. Although there are several recent examples of plasticity-first evolution in animals (e.g., [27–31]), further work on underrepresented organisms, like bacteria, is required to evaluate its general importance for adaptive evolution [32].

Here, we investigated the role of plasticity for adaptation to high temperature in the thermophilic, multicellular cyanobacterium *Fischerella* (also known as *Mastigocladus*). In the absence of a preferred nitrogen (N) source, these bacteria produce specialized N_2-fixing cells called heterocysts. Heterocysts differentiate from oxygen-evolving, carbon-fixing vegetative cells at semi-regular intervals through programmed morphological and physiological changes that protect the oxygen-sensitive and metabolically expensive N_2 fixation process [11, 12]. This includes the remodeling of the cell surface to form an envelope of glycolipid (heterocyst glycolipid [HG]) and polysaccharide (heterocyst envelope polysaccharide [HEP]) layers that acts as a non-selective barrier to gas diffusion [33, 34]. Both the HG and HEP layers of the heterocyst envelope are required for N_2 fixation in the presence of oxygen [35, 36], but the HG layer is considered to be the primary gas diffusion barrier [33]. For diverse heterocyst-forming cyanobacteria, HG composition is a plastic trait in both laboratory and natural environments that is determined by the temperature of development [13, 14]. Because a less-permeable envelope can mitigate the adverse effects of high temperature stress on heterocyst physiology [37], we suspected that the plasticity of HG composition may

tune a developing heterocyst to its current thermal environment by modulating its permeability.

We characterized the temperature dependence of HG composition for different *Fischerella* strains that have diverged in thermotolerance (Figure 1A; STAR Methods; Key Resources Table) [38] using high-performance liquid chromatography coupled to electrospray ionization tandem mass spectrometry (HPLC-ESI/MS^2). The glycolipid layer surrounding the heterocysts of these bacteria mainly consisted of four structural isomers of 1-(O-hexose)-3,29,31-dotriacontanetriol (HG_{32} triol) (Figure 1B; Table S1). In addition, minor quantities (mean ± SE = 0.7 ± 0.34%) of four structural isomers of 1-(O-hexose)-29-keto-3,31-dotriacontanediol (HG_{32} keto-diol) (Table S1) were observed in *Fischerella* strains grown at lower temperatures. Structural isomers differed solely in the identity and/or configuration of the hexose head group (Figure S1). These results are in agreement with other laboratory and field investigations of *Fischerella* [39, 40].

As observed for other cyanobacteria [13, 41], HG composition was temperature dependent for most *Fischerella* strains. The relative abundances of HG_{32} triol isomers II and IV increased at higher developmental temperatures (Figures 1B and 1C). Surprisingly, however, plasticity has been lost at least two times during the diversification of more thermotolerant *F. thermalis* strains, resulting in the constitutive overproduction of HG isomers that are associated with high developmental temperature in plastic strains (Figures 1C and 1D). One loss resulted in the exclusive synthesis of HG_{32} triol isomers II and IV by *F. thermalis* strains CCMEE 5192 (Chile) and CCMEE 5204 (Oman), which are identical in 16S rRNA gene sequence. A second loss of plasticity was observed for *F. thermalis* strain WC 559 (Yellowstone NP), which only produced isomers I and III in low quantities at 37°C (Figure 1D). In all cases, the reduction in plasticity is associated with maximal levels of high-temperature isomer abundance that were unattained by more plastic strains (Figure 1C). This maximal abundance was positively correlated with growth rate at high temperature (Figure 1E; R = 0.7; p = 0.025), which suggests that the loss of plasticity has contributed to the adaptation of some *Fischerella* strains to higher temperature environments.

Within-Population Variation in HG Composition Plasticity

To better understand the mechanisms and consequences of reduced HG composition plasticity for heterocyst function and organism fitness at high temperature, we sought to identify a *F. thermalis* population where individuals with reduced plasticity co-occur with and may be directly compared with close relatives that are ancestrally plastic. We focused on a set of strains from White Creek, an N-limited, geothermally heated stream in Yellowstone National Park from which strain WC 559 had been isolated [42]. At White Creek, *F. thermalis* forms streamer mats between 39°C and 54°C [42]. Strain WC 559 (Figure 1) belongs to the most abundant multi-locus haplotype (MLH3) at the upstream population boundary [42] and is a member of a distinct cluster of closely related White Creek *F. thermalis* referred to as group 2 strains [37].

Two additional MLH3 strains (WC 542 and WC 554) displayed a phenotype similar to WC 559, i.e., high relative abundance of HG_{32} triol isomers II and IV under all conditions and the complete loss of plasticity between 50°C and 55°C (Figure 2; Data S1). By contrast, other strains exhibited a high degree of plasticity (Figure 2; R^2 = 0.82 for a full factorial model of strain and temperature effects; p < 0.0001).

Consequences of Lower Plasticity for Heterocyst Function and Fitness

Is the loss of plasticity at White Creek locally adaptive at high temperature, and does it come with a performance cost in alternative environments? Although oxygen solubility decreases with an increase in temperature, protection of nitrogenase remains critical at higher temperature at White Creek. This is because the lower solubility is offset by the increase in the oxygen diffusion coefficient, and daytime oxygen concentrations are typically supersaturated within *F. thermalis* microbial mats [37]. We have previously shown that lower heterocyst permeability can help to maintain a micro-oxic environment within the heterocyst near the limit of *F. thermalis* thermotolerance [37]. However, plasticity of HG composition may tune heterocyst permeability to the temperature of development [13], thereby enabling rapid acclimation to changing environmental conditions. We tested whether the constitutive overproduction of high-temperature isomers by MLH3 strains results in a less-permeable heterocyst that can maintain N_2 fixation at high temperature but is deleterious at lower temperature. To do so, MLH3 strains and other group 2 strains were grown and assayed for N_2 fixation at either 37°C or 55°C, respectively. Only the HG isomer composition differed between the two sets of strains; glycolipid abundance itself (normalized to dry mass) did not (n = 18; $F_{11,6}$ = 1.55; p = 0.24), nor did it change with temperature (p = 0.23). Therefore, the evolution of MLH3 HG composition (Figure 2) occurred without an alteration of resource allocation to HG synthesis. This is important, because the heterocyst envelope is a serious investment of cellular resources, accounting for ~50% of cell dry weight [43].

To test whether MLH3 heterocysts are less permeable than those of other strains, we compared the light-independent (N_{dark}) and light-dependent ($N_{total} - N_{dark}$) components of N_2 fixation at 37°C. N_2 fixation in the dark is fueled by ATP provided by aerobic respiration, which in turn is controlled by oxygen diffusion into the heterocyst [34]. Consequently, we would expect a specific reduction in the light-independent component of N_2 fixation for a less permeable heterocyst. As predicted, N_2 fixation rates at 37°C were lower for MLH3 strains than for other group 2 strains but only for the light-independent component of N_2 fixation (Figure 3A; R^2 = 0.43, $F_{1,8}$ = 5.95, p < 0.05; p = 0.62 for the light-dependent component). In addition, the ATP limitation of nitrogenase activity in the dark, estimated by the ratio of total to dark N_2 fixation (N_{total}/N_{dark}) [34], was greater for MLH3 strains (mean ± SE: 11.5 ± 0.70) than for other group 2 strains (5.7 ± 0.48). MLH3 heterocysts therefore bear a cost at lower temperature. By contrast, total N_2 fixation rates (mean ± SE) of MLH3 strains were not inhibited at 55°C (126% ± 25.0% of 37°C rates; Figures 3A and 3B) but were only 63% ± 3.6% of 37°C rates for plastic group 2 strains (n = 6 strains; R^2 = 0.88; p = 0.01 for the strain type × temperature interaction). The latter strains showed a reduction in both light-dependent and light-independent N_2 fixation rates at 55°C compared with 37°C (Figures 3A and 3B). The more effective diffusion barrier of MLH heterocysts is therefore advantageous at higher temperature.

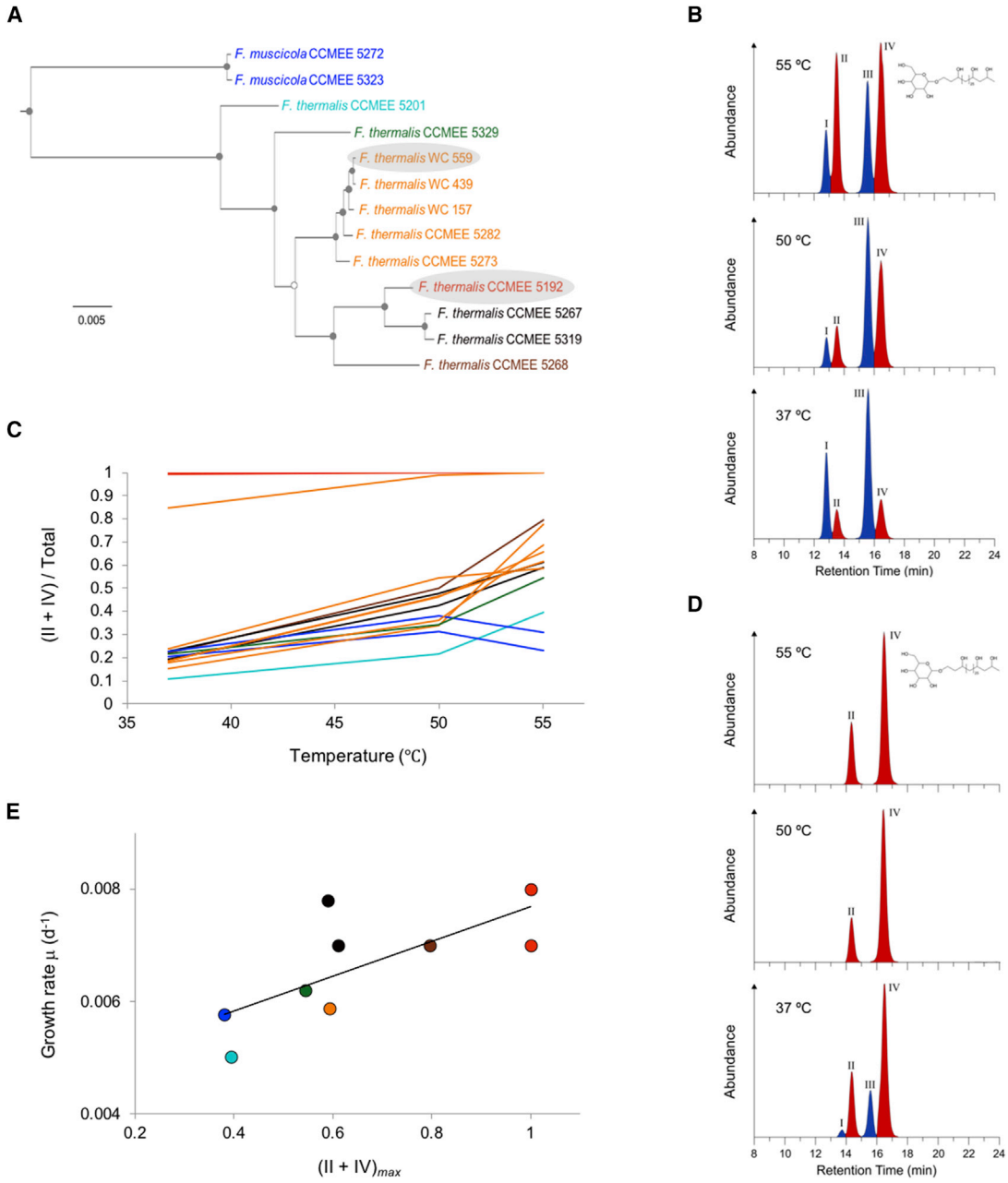

Figure 1. Plasticity of Heterocyst Glycolipid Composition Has Been Lost Multiple Times during *Fischerella* Evolution

(A) Maximum likelihood phylogeny of *Fischerella* strains reconstructed from a concatenated alignment of 2,877 protein-coding genes according to a mixture model of nucleotide substitution with gamma rate heterogeneity. Strains of *F. muscicola* and the basal *F. thermalis* strain CCMEE 5201 are less thermotolerant than other representatives of *F. thermalis*, indicating that more thermotolerant *Fischerella* evolved from less thermotolerant ancestors. Shaded strains have convergently lost plasticity for heterocyst glycolipid composition (see C). Bootstrap values of 100% (closed circles) and >95% (open circle) are indicated. The scale bar is in units of nucleotide substitutions per site.

(B) Representative HPLC chromatograms showing the relative distribution of structural isomers of HG_{32} triol (inset) at three temperatures for plastic *F. thermalis* strain WC 439. These structural isomers share the same aglycone moiety (see Figure S1). Glycolipid abundance data are provided in Table S1.

(C) The temperature dependence of the synthesis of HG_{32} triol isomers II and IV varies among *Fischerella* strains, with low-plasticity strains exhibiting constitutively high relative abundances. Color coding as in (A).

(D) HPLC chromatograms showing the reduction in the temperature dependence of HG_{32} triol composition for *F. thermalis* strain WC 559.

(E) *F. thermalis* strain growth rate at 50°C versus maximum production of HG_{32} triol isomers II and IV. Color coding as in (A). Growth rate data are from [38], and correlation analysis was conducted by phylogenetic generalized least-squares using the phylogenetic data in (A).

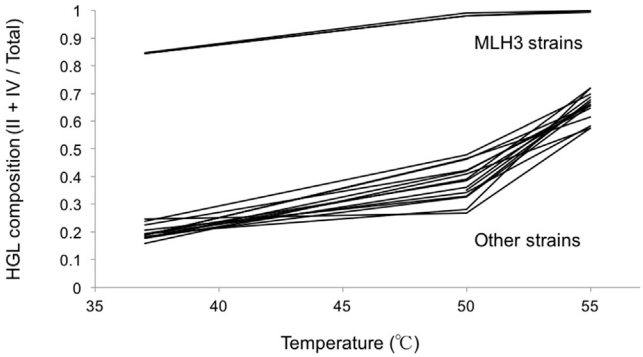

Figure 2. Only *F. thermalis* Strains with the MLH3 Haplotype Exhibit Reduced HG Composition Plasticity within the White Creek Population

Whereas most White Creek strains exhibited strong temperature dependence for the relative abundance of HG_{32} triol isomers II and IV, all three assayed strains with the MLH3 haplotype (WC 542, WC 554, and WC 559) have lost plasticity. Semiquantitative abundances are provided in Data S1.

MLH3 and plastic strains also differed in the temperature dependence of growth under heterocyst-forming conditions (Figure 3C; n = 30; R^2 = 0.39; p = 0.0002 for the strain type × temperature interaction). Whereas 55°C is stressful for plastic strains, MLH3 strains are high-temperature specialists (Figure 3C; n = 15; $F_{1,13}$ = 6.04; p < 0.03 for the strain type effect) that perform more poorly than other strains at 37°C ($F_{1,13}$ = 9.61; p < 0.01). However, this fitness advantage at 55°C was only observed if heterocysts were produced: growth rates of MLH3 and MLH6 strains (the most thermosensitive White Creek haplotype under N_2-fixing conditions) [42] were not significantly different when a more preferred N source (nitrate) was available in the environment (Figure 3D; n = 3 strains each; p = 0.43 for the haplotype × time interaction). We conclude that the constitutive reduction of heterocyst diffusion barrier efficiency in MLH3 strains is locally adaptive in high-temperature, N-limited environments, but it comes at the cost of ecological specialization due to its pleiotropic effects on heterocyst function at physiological extremes.

Population Genomics of Lost Plasticity

How are MLH3 strains genetically different from plastic strains? Using previously available [37] and newly acquired genome data (including data for eight MLH3 strains), we observed that the genomes of MLH3 strains are nearly identical to each other and to other group 2 strains (Figure 4A). In a genome-wide scan of genetic differentiation (Φ_{ST}) for 2,011 polymorphic protein-coding genes, MLH3 strains were fixed for a different nucleotide than other White Creek strains at only 48 SNP sites distributed throughout the ~5.4-Mbp genome (Figure 4B; Table S2). Of these, two are located in genes known to be involved in heterocyst development and function (Table S2). One is a synonymous SNP in *hepB* (Table S2), which encodes a glycosyltransferase required for HEP formation [44] but is not known to be involved in the synthesis of the HG layer. By contrast, the most promising candidate associated with the loss of HG plasticity is a non-synonymous SNP in *hglT* (Table S2). This gene is located within the expression island that is responsible for the production of the glycolipid layer of the heterocyst envelope [35, 45] and encodes a glycosyltransferase that has been shown to glycosylate aglycones to form mature heterocyst glycolipids [46]. A sliding window analysis of the region revealed this to be the only fixed

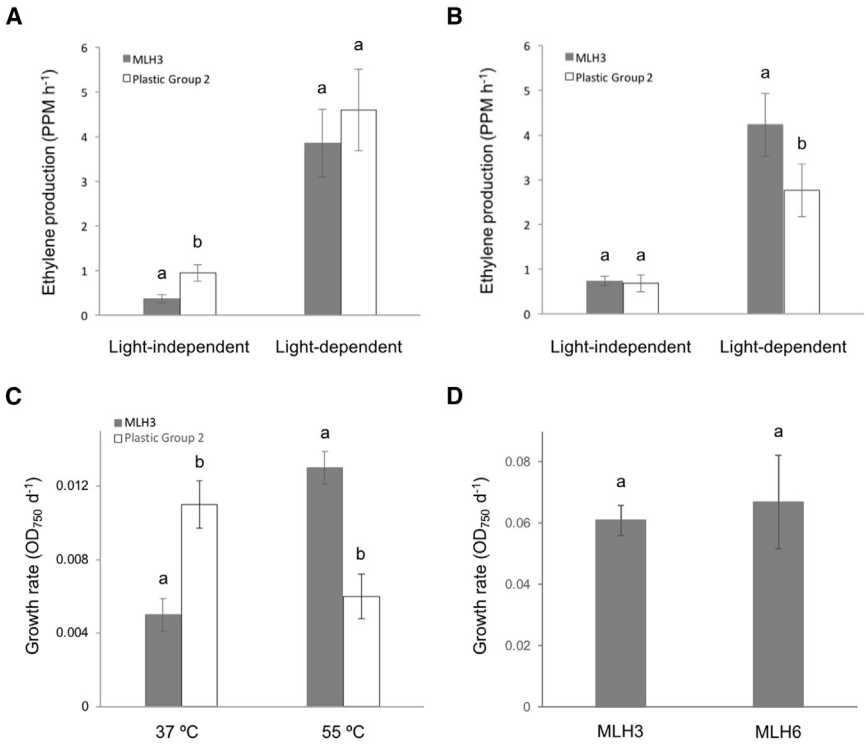

Figure 3. *F. thermalis* MLH3 Strains Are High-Temperature Specialists with Reduced Nitrogen Fixation Activity and Fitness at Lower Temperature

(A and B) Light-independent (dark) and light-dependent (total − dark) contributions to nitrogen fixation were measured as cell-normalized ethylene production at 37°C (A) and 55°C (B) for both MLH3 and other group 2 *F. thermalis* strains. Strains were grown at the respective assay temperatures. Error bars indicate SEs. Different letters within an experimental treatment indicate a significant difference by t test at the p < 0.05 level.

(C) Growth rates of MLH3 strains versus other White Creek strains were estimated at 37°C and 55°C, respectively. Error bars indicate SEs. Data are from [42]. Different letters within an experimental treatment indicate a significant difference by t test at the p < 0.05 level.

(D) Growth rates of MLH3 versus MLH6 strains at 55°C when grown with nitrate as nitrogen source. Heterocysts were not produced under these conditions. Error bars indicate SEs.

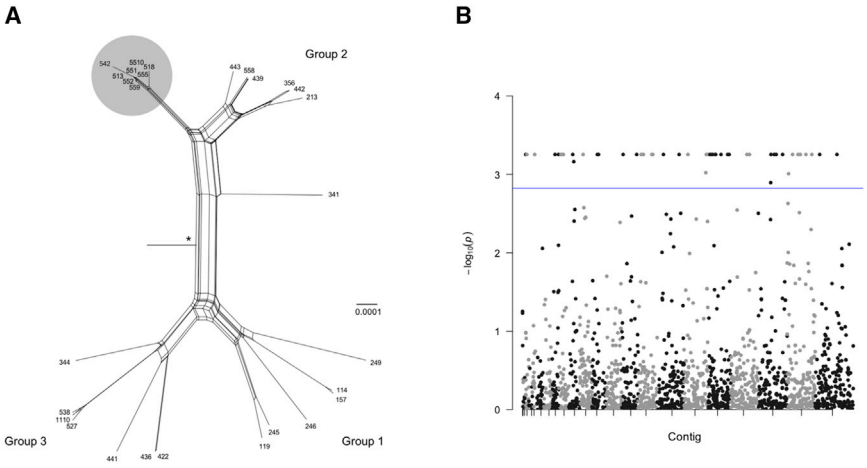

Figure 4. Plasticity of *F. thermalis* MLH3 Strains Was Lost Recently

(A) Neighbor net analysis of the relationships among 28 White Creek *F. thermalis* strains for a concatenated alignment of 2,057,562 nucleotides reveals MLH3 strains (shaded in gray) to be a recently derived lineage within group 2 *F. thermalis*. The most recent common ancestor of the White Creek population is indicated by an asterisk. The scale bar is in units of nucleotide substitutions per site.

(B) Manhattan plot of the log-transformed significance values of Φ_{ST} genetic differentiation estimates between MLH3 and other strains for 2,011 polymorphic protein-coding genes, mapped to the *F. thermalis* strain JSC-11 reference genome assembly. Only 53 genes exceeded the significance threshold with a false discovery rate q value of 5% (indicated by the blue line), 48 of which were completely differentiated between MLH3 and other strains (see Table S2 and Figure S2 for details).

difference in the HG expression island between plastic and MLH3 strains (Figure S2). A comparison with genome data available for *Fischerella* strains from around the world (Figure 1A) further demonstrated that this SNP is not observed in any other genome. This indicates that the *hglT* SNP was likely derived at White Creek during the divergence of MLH3 from other group 2 strains. It also implies that the convergent loss of plasticity in other *F. thermalis* strains has a different genetic basis. Transformation and conjugal transfer methods have been recently developed for *F. muscicola* [47, 48], and future work will aim to take a genetic approach to determine whether and how the *hglT* SNP contributes to differences in HG isomer abundance.

Plasticity-First Evolution and the Origins of Cellular Innovation

Evolutionary changes in cell design and performance can be a source of new adaptive traits and biological diversity, but the processes by which this happens are not clear [1]. Our study implicates a role for the genetic assimilation of developmental plasticity for the adaptive molecular evolution of the cell. This is in accord with key predictions of the plasticity-first hypothesis that natural selection may change and refine the environmental dependence of a genetically variable, ancestrally plastic trait under novel conditions [4].

HG composition is an ancestrally plastic trait [13, 41], and this plastic ancestry is reflected in the residual production of low amounts of low-temperature HG isomers by *F. thermalis* MLH3 strains at 37°C (Figure 2). The loss of phenotypic plasticity of HG isomer composition (Figure 1) would be expected to be deleterious in a heterogeneous environment, where individuals may experience a broad range of environmental conditions. By contrast, reduced environmental variation may promote the chance or selectively favored loss of plasticity, a phenomenon that has been described for experimentally evolved bacterial populations maintained in a constant environment [49]. We speculate that selection to maintain plasticity may have been relaxed at the upstream boundary of the White Creek *F. thermalis* population, where environmental temperature is much less variable compared with downstream sites (coefficients of variation of 2% versus 5%) [42]. This may have set the stage for adaptation.

Plastic *Fischerella* strains were never observed to exclusively produce high-temperature HG isomers at higher temperatures (Figures 1C and 2), even though it would be beneficial to do so (Figure 3). It is not clear why plastic strains do not better match their environment under high-temperature stress. Potentially, a developmental range constraint may prevent them from producing a more extreme phenotype [17]. In any case, this observation suggests that the loss of HG composition plasticity was favored in a stable mis-matched environment. This loss of plasticity at White Creek appears to have a simple genetic basis involving new mutation(s) (Figure 4). This is in agreement with recent support for the role of mutation as a mechanism of genetic assimilation in a stressful environment [50] rather than from standing cryptic variation revealed under stress, as originally envisioned [20].

Our study illustrates how evolved modifications of plastic variation at the cellular level can promote local adaptation and ecological specialization. Further tests are needed to determine how pervasive a role phenotypic plasticity plays in the adaptive diversification of cells, but the repeatable nature of this process for heterocyst evolution during *Fischerella* diversification suggests that adaptation from plasticity may potentially be of general importance for other environmentally inducible cellular traits, e.g., cytoplasmic membrane composition.

STAR★METHODS

Detailed methods are provided in the online version of this paper and include the following:

- KEY RESOURCES TABLE
- LEAD CONTACT AND MATERIALS AVAILABILITY
- EXPERIMENTAL MODEL AND SUBJECT DETAILS
  - Fischerella
- METHOD DETAILS
  - Fischerella growth for heterocyst glycolipid analysis

SUPPLEMENTAL INFORMATION

Supplemental Information can be found online at https://doi.org/10.1016/j.cub.2019.11.056.

ACKNOWLEDGMENTS

We thank the Cory Cleveland laboratory group (University of Montana) for use of their gas chromatograph to determine nitrogen fixation rates. We also thank the two anonymous reviewers for their comments, which greatly improved the paper. Collections of *F. thermalis* from White Creek were supported by Yellowstone National Park research permit YELL-5482. T.B. acknowledges J. Weber for laboratory assistance during sample preparation and extraction. This work was supported by US National Science Foundation award IOS-1110819 and by National Aeronautics and Space Administration award NNA15BB04A to S.R.M.

AUTHOR CONTRIBUTIONS

Conceptualization, S.R.M. and T.B.; Methodology, S.R.M. and T.B.; Investigation, S.R.M., T.B., R.L., and P.R.H.; Writing – Original Draft, S.R.M. and T.B.; Writing – Review & Editing, S.R.M., T.B., R.L., and P.R.H.; Funding Acquisition, S.R.M.; Resources, S.R.M. and T.B.; Supervision, S.R.M. and T.B.

DECLARATION OF INTERESTS

The authors declare no competing interests.

Received: September 27, 2019
Revised: November 12, 2019
Accepted: November 18, 2019
Published: January 9, 2020

REFERENCES

1. Lynch, M., Field, M.C., Goodson, H.V., Malik, H.S., Pereira-Leal, J.B., Roos, D.S., Turkewitz, A.P., and Sazer, S. (2014). Evolutionary cell biology: two origins, one objective. Proc. Natl. Acad. Sci. USA *111*, 16990–16994.
2. West-Eberhard, M.J. (2003). Developmental Plasticity and Evolution (Oxford University Press).
3. Schwander, T., and Leimar, O. (2011). Genes as leaders and followers in evolution. Trends Ecol. Evol. *26*, 143–151.
4. Levis, N.A., and Pfennig, D.W. (2016). Evaluating "plasticity-first" evolution in nature: key criteria and empirical approaches. Trends Ecol. Evol. *31*, 563–574.
5. Via, S., and Lande, R. (1985). Genotype-environment interaction and the evolution of phenotypic plasticity. Evolution *39*, 505–522.
6. Via, S., Gomulkiewicz, R., De Jong, G., Scheiner, S.M., Schlichting, C.D., and Van Tienderen, P.H. (1995). Adaptive phenotypic plasticity: consensus and controversy. Trends Ecol. Evol. *10*, 212–217.
7. Schlichting, C.D., and Pigliucci, M. (1998). Phenotypic Evolution: a Reaction Norm Perspective (Sinauer Assocs., Inc.).
8. Price, T.D., Qvarnström, A., and Irwin, D.E. (2003). The role of phenotypic plasticity in driving genetic evolution. Proc. Biol. Sci. *270*, 1433–1440.
9. Wund, M.A. (2012). Assessing the impacts of phenotypic plasticity on evolution. Integr. Comp. Biol. *52*, 5–15.
10. Laland, K., Uller, T., Feldman, M., Sterelny, K., Müller, G.B., Moczek, A., Jablonka, E., Odling-Smee, J., Wray, G.A., Hoekstra, H.E., et al. (2014). Does evolutionary theory need a rethink? Nature *514*, 161–164.
11. Herrero, A., Stavans, J., and Flores, E. (2016). The multicellular nature of filamentous heterocyst-forming cyanobacteria. FEMS Microbiol. Rev. *40*, 831–854.
12. Flores, E., Picossi, S., Valladares, A., and Herrero, A. (2019). Transcriptional regulation of development in heterocyst-forming cyanobacteria. Biochim. Biophys. Acta. Gene Regul. Mech. *1862*, 673–684.
13. Bauersachs, T., Stal, L.J., Grego, M., and Schwark, L. (2014). Temperature induced changes in the heterocyst glycolipid composition of N_2 fixing heterocystous cyanobacteria. Org. Geochem. *69*, 98–105.
14. Bauersachs, T., Rochelmeier, J., and Schwark, L. (2015). Seasonal lake surface water temperature trends reflected by heterocyst glycolipid-based molecular thermometers. Biogeosci. *12*, 3741–3751.
15. Van Tienderen, P.H. (1991). Evolution of generalists and specialists in spatially heterogeneous environments. Evolution *45*, 1317–1331.
16. Moran, N.A. (1992). The evolutionary maintenance of alternative phenotypes. Am. Nat. *139*, 971–989.
17. Dewitt, T.J., Sih, A., and Wilson, D.S. (1998). Costs and limits of phenotypic plasticity. Trends Ecol. Evol. *13*, 77–81.
18. Murren, C.J., Auld, J.R., Callahan, H., Ghalambor, C.K., Handelsman, C.A., Heskel, M.A., Kingsolver, J.G., Maclean, H.J., Masel, J., Maughan, H., et al. (2015). Constraints on the evolution of phenotypic plasticity: limits and costs of phenotype and plasticity. Heredity *115*, 293–301.
19. Schmalhausen, I.I. (1949). Factors of Evolution (Blakiston Company).
20. Waddington, C.H. (1961). Genetic assimilation. Adv. Genet. *10*, 257–293.
21. Pigliucci, M., Murren, C.J., and Schlichting, C.D. (2006). Phenotypic plasticity and evolution by genetic assimilation. J. Exp. Biol. *209*, 2362–2367.
22. Futuyma, D.J., and Moreno, G. (1988). The evolution of ecological specialization. Annu. Rev. Ecol. Syst. *19*, 207–233.
23. Lynch, M., and Lande, R. (1993). Evolution and extinction in response to environmental change. In Biotic Interactions and Global Change, P. Kareiva, J. Kingsolver, and R. Huey, eds. (Sinauer Assocs., Inc.), pp. 234–250.
24. Poisot, T., Bever, J.D., Nemri, A., Thrall, P.H., and Hochberg, M.E. (2011). A conceptual framework for the evolution of ecological specialisation. Ecol. Lett. *14*, 841–851.
25. Badyaev, A.V. (2005). Stress-induced variation in evolution: from behavioural plasticity to genetic assimilation. Proc. Biol. Sci. *272*, 877–886.
26. Wagner, G.P., Erkenbrack, E.M., and Love, A.C. (2019). Stress-induced evolutionary innovation: a mechanism for the origin of cell types. BioEssays *41*, e1800188.
27. Levis, N.A., Isdaner, A.J., and Pfennig, D.W. (2018). Morphological novelty emerges from pre-existing phenotypic plasticity. Nat. Ecol. Evol. *2*, 1289–1297.
28. Bock, D.G., Kantar, M.B., Caseys, C., Matthey-Doret, R., and Rieseberg, L.H. (2018). Evolution of invasiveness by genetic accommodation. Nat. Ecol. Evol. *2*, 991–999.
29. Corl, A., Bi, K., Luke, C., Challa, A.S., Stern, A.J., Sinervo, B., and Nielsen, R. (2018). The genetic basis of adaptation following plastic changes in coloration in a novel environment. Curr. Biol. *28*, 2970–2977.e7.
30. Kulkarni, S.S., Denver, R.J., Gomez-Mestre, I., and Buchholz, D.R. (2017). Genetic accommodation via modified endocrine signalling explains phenotypic divergence among spadefoot toad species. Nat. Commun. *8*, 993.
31. Scoville, A.G., and Pfrender, M.E. (2010). Phenotypic plasticity facilitates recurrent rapid adaptation to introduced predators. Proc. Natl. Acad. Sci. USA *107*, 4260–4263.

32. Levis, N.A., and Pfennig, D.W. (2019). Plasticity-led evolution: a survey of developmental mechanisms and empirical tests. Evol. Dev. https://doi.org/10.1111/ede.12309.
33. Walsby, A.E. (1985). The permeability of heterocysts to the gases nitrogen and oxygen. Proc. R. Soc. Lond. B Biol. Sci. *226*, 345–366.
34. Staal, M., Meysman, F.J., and Stal, L.J. (2003). Temperature excludes N_2-fixing heterocystous cyanobacteria in the tropical oceans. Nature *425*, 504–507.
35. Fan, Q., Huang, G., Lechno-Yossef, S., Wolk, C.P., Kaneko, T., and Tabata, S. (2005). Clustered genes required for synthesis and deposition of envelope glycolipids in *Anabaena* sp. strain PCC 7120. Mol. Microbiol. *58*, 227–243.
36. Huang, G., Fan, Q., Lechno-Yossef, S., Wojciuch, E., Wolk, C.P., Kaneko, T., and Tabata, S. (2005). Clustered genes required for the synthesis of heterocyst envelope polysaccharide in *Anabaena* sp. strain PCC 7120. J. Bacteriol. *187*, 1114–1123.
37. Sano, E.B., Wall, C.A., Hutchins, P.R., and Miller, S.R. (2018). Ancient balancing selection on heterocyst function in a cosmopolitan cyanobacterium. Nat. Ecol. Evol. *2*, 510–519.
38. Miller, S.R., Castenholz, R.W., and Pedersen, D. (2007). Phylogeography of the thermophilic cyanobacterium *Mastigocladus laminosus*. Appl. Environ. Microbiol. *73*, 4751–4759.
39. Bauersachs, T., Miller, S.R., van der Meer, M.T.J., Hopmans, E.C., Schouten, S., and Sinninghe Damsté, J.S. (2013). Distribution of long chain heterocyst glycolipids in cultures of the thermophilic cyanobacterium *Mastigocladus laminosus* and a hot spring microbial mat. Org. Geochem. *56*, 19–24.
40. Bauersachs, T., Miller, S.R., Gugger, M., Mudimu, O., Friedl, T., and Schwark, L. (2019). Heterocyte glycolipids indicate polyphyly of stigonematalean cyanobacteria. Phytochemistry *166*, 112059.
41. Bauersachs, T., Compaoré, J., Hopmans, E.C., Stal, L.J., Schouten, S., and Sinninghe Damsté, J.S. (2009). Distribution of heterocyst glycolipids in cyanobacteria. Phytochemistry *70*, 2034–2039.
42. Miller, S.R., Williams, C., Strong, A.L., and Carvey, D. (2009). Ecological specialization in a spatially structured population of the thermophilic cyanobacterium *Mastigocladus laminosus*. Appl. Environ. Microbiol. *75*, 729–734.
43. Dunn, J.H., and Wolk, C.P. (1970). Composition of the cellular envelopes of *Anabaena cylindrica*. J. Bacteriol. *103*, 153–158.
44. Maldener, I., Hannus, S., and Kammerer, M. (2003). Description of five mutants of the cyanobacterium Anabaena sp strain PCC 7120 affected in heterocyst differentiation and identification of the transposon-tagged genes. FEMS Microbiol. Lett. *224*, 205–213.
45. Ehira, S., Ohmori, M., and Sato, N. (2003). Genome-wide expression analysis of the responses to nitrogen deprivation in the heterocyst-forming cyanobacterium *Anabaena* sp. strain PCC 7120. DNA Res. *10*, 97–113.
46. Awai, K., and Wolk, C.P. (2007). Identification of the glycosyl transferase required for synthesis of the principal glycolipid characteristic of heterocysts of *Anabaena* sp. strain PCC 7120. FEMS Microbiol. Lett. *266*, 98–102.
47. Stucken, K., Ilhan, J., Roettger, M., Dagan, T., and Martin, W.F. (2012). Transformation and conjugal transfer of foreign genes into the filamentous multicellular cyanobacteria (subsection V) *Fischerella* and *Chlorogloeopsis*. Curr. Microbiol. *65*, 552–560.
48. Antonaru, L.A., and Nürnberg, D.J. (2017). Role of PatS and cell type on the heterocyst spacing pattern in a filamentous branching cyanobacterium. FEMS Microbiol. Lett. *364*, fnx154.
49. Maughan, H., Masel, J., Birky, C.W., Jr., and Nicholson, W.L. (2007). The roles of mutation accumulation and selection in loss of sporulation in experimental populations of *Bacillus subtilis*. Genetics *177*, 937–948.
50. Fanti, L., Piacentini, L., Cappucci, U., Casale, A.M., and Pimpinelli, S. (2017). Canalization by selection of *de Novo* induced mutations. Genetics *206*, 1995–2006.
51. Nguyen, L.T., Schmidt, H.A., von Haeseler, A., and Minh, B.Q. (2015). IQ-TREE: a fast and effective stochastic algorithm for estimating maximum-likelihood phylogenies. Mol. Biol. Evol. *32*, 268–274.
52. Whitlock, M.C., and Lotterhos, K.E. (2015). Reliable detection of loci responsible for local adaptation: inference of a null model through trimming the distribution of F(ST). Am. Nat. *186* (*Suppl 1*), S24–S36.
53. Librado, P., and Rozas, J. (2009). DnaSP v5: a software for comprehensive analysis of DNA polymorphism data. Bioinformatics *25*, 1451–1452.
54. Bolger, A.M., Lohse, M., and Usadel, B. (2014). Trimmomatic: a flexible trimmer for Illumina sequence data. Bioinformatics *30*, 2114–2120.
55. Zerbino, D.R., and Birney, E. (2008). Velvet: algorithms for de novo short read assembly using de Bruijn graphs. Genome Res. *18*, 821–829.
56. Castenholz, R.W. (1988). Culturing methods for cyanobacteria. Methods Enzymol. *167*, 68–93.
57. Bligh, E.G., and Dyer, W.J. (1959). A rapid method of total lipid extraction and purification. Can. J. Biochem. Physiol. *37*, 911–917.
58. Rütters, H., Sass, H., Cypionka, H., and Rullkötter, J. (2002). Phospholipid analysis as a tool to study complex microbial communities in marine sediments. J. Microbiol. Methods *48*, 149–160.
59. Bauersachs, T., Talbot, H.M., Sidgwick, F., Sivonen, K., and Schwark, L. (2017). Lipid biomarker signatures as tracers for harmful cyanobacterial blooms in the Baltic Sea. PLoS ONE *12*, e0186360.
60. Bauersachs, T., Hopmans, E.C., Compaoré, J., Stal, L.J., Schouten, S., and Damsté, J.S. (2009). Rapid analysis of long-chain glycolipids in heterocystous cyanobacteria using high-performance liquid chromatography coupled to electrospray ionization tandem mass spectrometry. Rapid Commun. Mass Spectrom. *23*, 1387–1394.
61. Bryce, T.A., Welti, D., Walsby, A.E., and Nichols, B.W. (1972). Monohexoside derivatives of long-chain polyhydroxy alcohols; a novel class of glycolipid specific to heterocystous algae. Phytochemistry *11*, 295–302.
62. Inskeep, W.P., Jay, Z.J., Tringe, S.G., Herrgård, M.J., and Rusch, D.B.; YNP Metagenome Project Steering Committee and Working Group Members (2013). The YNP metagenome project: environmental parameters responsible for microbial distribution in the Yellowstone geothermal ecosystem. Front. Microbiol. *4*, 67.
63. Stewart, W.D.P., Fitzgerald, G.P., and Burris, R.H. (1967). In situ studies on N_2 fixation using the acetylene reduction technique. Proc. Natl. Acad. Sci. USA *58*, 2071–2078.
64. Hutchins, P.R., and Miller, S.R. (2017). Genomics of variation in nitrogen fixation activity in a population of the thermophilic cyanobacterium *Mastigocladus laminosus*. ISME J. *11*, 78–86.

STAR★METHODS

KEY RESOURCES TABLE

REAGENT or RESOURCE	SOURCE	IDENTIFIER
Bacterial and Virus Strains		
Fischerella muscicola strain CCMEE 5272	[38]	N/A
Fischerella muscicola strain CCMEE 5323	[38]	N/A
Fischerella thermalis strain CCMEE 5201	[38]	N/A
Fischerella thermalis strain CCMEE 5329	[38]	N/A
Fischerella thermalis strain CCMEE 5282	[38]	N/A
Fischerella thermalis strain CCMEE 5273	[38]	N/A
Fischerella thermalis strain CCMEE 5192	[38]	N/A
Fischerella thermalis strain CCMEE 5267	[38]	N/A
Fischerella thermalis strain CCMEE 5319	[38]	N/A
Fischerella thermalis strain CCMEE 5268	[38]	N/A
Fischerella thermalis strain WC 114	[42]	N/A
Fischerella thermalis strain WC 116	[42]	N/A
Fischerella thermalis strain WC 119	[42]	N/A
Fischerella thermalis strain WC 1110	[42]	N/A
Fischerella thermalis strain WC 157	[42]	N/A
Fischerella thermalis strain WC 213	[42]	N/A
Fischerella thermalis strain WC 217	[42]	N/A
Fischerella thermalis strain WC 245	[42]	N/A
Fischerella thermalis strain WC 246	[42]	N/A
Fischerella thermalis strain WC 249	[42]	N/A
Fischerella thermalis strain WC 439	[42]	N/A
Fischerella thermalis strain WC 441	[42]	N/A
Fischerella thermalis strain WC 527	[42]	N/A
Fischerella thermalis strain WC 538	[42]	N/A
Fischerella thermalis strain WC 542	[42]	N/A
Fischerella thermalis strain WC 554	[42]	N/A
Fischerella thermalis strain WC 558	[42]	N/A
Fischerella thermalis strain WC 559	[42]	N/A
Chemicals, Peptides, and Recombinant Proteins		
2-Propanol	Roth	AE73.2; CAS: 67-63-0
Ammonia solution 25%	Merck	5.33003.0050
Dichloromethane	Merck	1.06044.2500; CAS: 75-09-2
Formic Acid 98-100%	Merck	1.00264.1000; CAS: 64-18-6
Methanol	Roth	HN41.2; CAS: 67-56-1
n-Hexane	Merck	1.03701.2500; CAS: 110-54-3
Potassium phosphate dibasic	Sigma-Aldrich	P3786; CAS: 7758-11-4
Water	VWR Chemicals	23595.328; CAS: 7732-18-5
Deposited Data		
Fischerella genome sequence data	This study	NCBI BioProject: PRJNA322208
Software and Algorithms		
Sequence Matrix	https://github.com/gaurav/taxondna	V1.8
IQ-TREE	[51]	V1.55
SplitsTree	http://www.splitstree.org	V4.14.4

(*Continued on next page*)

Continued

REAGENT or RESOURCE	SOURCE	IDENTIFIER
OutFLANK	[52]	V0.2
qqman	https://cran.r-project.org/web/packages/qqman	V0.1.4
DNASP	[53]	V5.10
COMPARE	http://www.indiana.edu/~martinsl/compare/v46b/compare	V4.6b
Trimmomatic	[54]	V0.22
Velvet	[55]	V1.2.03
JMP	https://www.jmp.com	V10
MassLynx	https://www.waters.com	V4.1
QuanLynx	https://www.waters.com	V4.1

LEAD CONTACT AND MATERIALS AVAILABILITY

Further information and requests for resources and reagents should be directed to and will be fulfilled by the Lead Contact, Scott Miller (scott.miller@umontana.edu). This study did not generate any new unique reagents.

EXPERIMENTAL MODEL AND SUBJECT DETAILS

Fischerella

Fischerella strains were routinely maintained as batch cultures in 75 mL of D medium [56] at 50°C, on a 12 h/12 h (light-dark) cycle and at a light intensity of 75 μmol photons m^{-2} s^{-1} of cool white fluorescent light. D medium consists of the following dissolved in 1 L distilled water (with pH adjusted to 8.2 to NaOH prior to autoclaving): 100.0 mg nitrilotriacetic acid; 60.0 mg $CaSO_4$ x 2 H_2O; 100.0 mg $MgSO_4$ x 7 H_2O; 8.0 mg NaCl 8.00; 103 mg KNO_3; 689.0 mg $NaNO_3$; 140.0 mg Na_2HPO_4 x 2 H_2O; 0.47 mg $FeCl_3$ x 6 H_2O ; 2.20 mg $MnSO_4$ x H_2O; 0.50 mg $ZnSO_4$ x 7 H_2O; 0.50 mg H_3BO_3; 25.0 mg $CuSO_4$ x 5 H_2O; 25.0 μg Na_2MoO_4 x 2 H_2O; and 46.0 μg $CoCl_2$ x 6 H_2O.

METHOD DETAILS

Fischerella growth for heterocyst glycolipid analysis

White Creek *F. thermalis* strains were grown as batch cultures in 350 mL of ND medium (medium D [56] without combined N) to induce formation of heterocysts. For each strain, three different cultures were maintained at 37, 50 and 55°C, respectively, on a 12 h/12 h (light-dark) cycle and at a light intensity of 75 μmol photons m^{-2} s^{-1} of cool white fluorescent light. Growing cells were pelleted, washed with sterile double distilled water, freeze-dried and stored at −20°C until shipped on dry ice to Christian-Albrechts-University for HG analysis.

Heterocyst glycolipid analysis

Cell material was extracted using a modified Bligh and Dyer technique [57, 58]. Between 5 and 16 mg of cell material was extracted ultrasonically (× 3) for 10 min in a solvent mixture of methanol (MeOH), dichloromethane (DCM) and phosphate buffer (2:1:0.8, v:v:v). After sonication, the combined extracts were phase-separated by adding DCM and phosphate buffer to a solvent ration of 1:1:0.9 (v:v:v). The bottom layer, containing HGs and other intact polar lipids, was collected and the aqueous phase re-extracted thrice with DCM. The bulk of the supernatant was removed by rotary evaporation and the obtained Bligh and Dyer extracts (BDEs) dried under a gentle stream of N_2. Each BDE was re-dissolved in a solvent mixture of hexane:2-propanol:H_2O (72:27:1, v:v:v) to a concentration of 0.5 mg ml^{-1} and aliquots were passed through 0.45 μm regenerated cellulose syringe filters prior to analysis. Heterocyst glycolipids were analyzed using high performance liquid chromatography coupled to tandem mass spectrometry (HPLC-ESI/MS^2) as reported previously [59]. Briefly, aliquots of the filtered BDEs were injected into a Waters Alliance 2690 HPLC system fitted with a Phenomenex Luna NH_2 column (150 × 2 mm; 3 μm particle size) and a guard column of the same material. Separation of target compounds was achieved at 30°C and using the following gradient profile: 95% A/5% B to 85% A/15% B in 10 min (held 7 min) at 0.5 mL min^{-1}, followed by back flushing with 30% A/ 70% B at 0.2 mg ml^{-1} for 25 min and re-equilibrating the column with 95% A/5% B for 15 min. Solvent A was *n*-hexane:2-propanol:HCO_2H:14.8 M NH_3 aq. (79:20:0.12:0.04, v:v:v:v) and solvent B was 2-propanol:H_2O:HCO_2H:14.8 M NH_3 aq. (88:10:0.12:0.04, v:v:v:v). Detection of HGs was achieved using a Micromass Quattro LC triple quadrupole mass spectrometer equipped with an electrospray ionization (ESI) interface that was operated in positive ion mode. Source conditions were as follows: capillary 3.5 kV, cone 20 V, desolvation temperature 230°C, source 120°C; cone gas

70 l h^{-1} and desolvation gas 230 l h^{-1}. BDEs were screened in data-dependent mode with two scan events, where a scan of *m/z* 300 to 1000 was followed by a product ion scan of the base peak in the spectrum of the first scan event. Structural assignment of HGs was achieved by comparison of mass spectra published in the literature [39, 60]. In order to facilitate an improved detection of those HG_{32} triol and HG_{32} keto-diol isomers, which occurred in only low quantities in *F. thermalis* strains, all samples were re-analyzed in multiple reaction monitoring (MRM) mode using the following transitions *m/z* 677 → 515 (HG_{32} triol) and *m/z* 675 → 513 (HG_{32} keto-diol). To allow semiquantitative estimates of HG abundances, all BDEs were dissolved to the same concentration and peak areas normalized to the amount of dry biomass (see Data S1).

Analysis of HG aglycone moieties

In order to determine the structure of the aglycone moiety of the heterocyst glycolipids present in *F. thermalis* strains, we subjected an aliquot of the freeze-dried cell material (~30 mg) to acid hydrolysis as described in Bauersachs et al. [60]. Briefly, the biomass was transferred to a centrifuge vial and reacted with a solvent mixture of 2 M HCl:MeOH (1:1, v:v) for 4 h at 85°C. After cooling to room temperature, the pH was adjusted to 3 by adding a solution of 2 M methanolic KOH. After centrifugation (4700 × g, 10 min), the supernatant was collected and the residuum extracted twice with MeOH in an ultrasonic bath (10 min). Subsequently, DCM and HPLC-grade water was added to the pooled extracts to achieve phase separation. The organic bottom layer was collected and the remaining MeOH/aqueous phase washed twice with DCM. Thereafter, the hydrolyzed extract was dried under a stream of N_2 and separated into hydrocarbon, fatty acid and alcohol fractions using activated aluminum oxide (Al_2O_3) as stationary phase and hexane:DCM (95:5, v:v), hexane:DCM (1:2, v:v) and DCM:MeOH (1:1, v:v) as respective solvents. The alcohol fraction, containing the HG-derived aglycone moieties, was dried under N_2 gas, re-dissolved in DCM to a concentration of 2 mg ml^{-1} and reacted with N,O-bis(trimethylsilyl)trifluoroacetamide (BSTFA) in the presence of pyridine for 1 h at 60°C prior to analysis by gas chromatography coupled to mass spectrometry (GC-MS).

GC-MS analysis was achieved using an Agilent 7820A gas chromatograph fitted with a Phenomenex ZB-5 fused silica column (30 m × 0.25 mm i.d.; 0.25 μm film thickness). Helium was used a carrier gas with a constant flow of 1 mL min^{-1}. The injector temperature was held at 70°C and the oven ramped from 70°C to 130°C at 20°C min^{-1} and then at 5°C min^{-1} to 320°C, after which the temperature was held isothermal for 20 min. The GC was interfaced with an Agilent 5975 MSD mass spectrometer operated at 70 eV and scanning *m/z* 50 to 850 with a cycle time of 1.7 s (resolution 1000). Identification of aglycone moieties was achieved by comparison of mass spectral characteristics with those published in the literature [60, 61].

Phylogenetic analysis

Orthologous protein-coding genes were identified and aligned for published genome data from thirteen *Fischerella* strains (NCBI BioProject: PRJNA322208 [37];) using custom Perl scripts (http://www.nature.com/ismej/journal/v11/n1/abs/ismej2016105a.html). A concatenated DNA sequence alignment was then produced with Sequence Matrix version 1.8 for the 2,877 protein-coding genes (2,165,499 nucleotides) for which sequence data were available for at least twelve strains. This sequence alignment was used to infer a maximum likelihood phylogeny and 1,000 ultrafast bootstrap replicates with IQ-TREE version 1.5.5 [51]. We used a mixture model of DNA substitution (HKY and GTR models) with rate heterogeneity (a discrete approximation of a gamma distribution with four rate categories), for a total of eight possible mixture classes (the product of the two substitution models and four gamma rate categories). For each nucleotide position in the alignment, the probability of belonging to each class was computed as part of the analysis.

Genome sequencing, assembly and annotation

Genomic DNA was extracted from *Fischerella* strains as described in Inskeep et al. [62] and sent to the University of Pittsburgh Center for Evolutionary Genomics Research for library preparation and 151-bp paired-end sequencing on an Illumina NextSeq 500 flow cell. Sequence reads were trimmed of leading and trailing low-quality bases and ambiguous nucleotides as well as filtered based on read length and sequence quality with Trimmomatic version 0.22 [54]. Draft genome assemblies for each strain were subsequently obtained with Velvet version 1.2.03 [55] using parameter settings that were manually optimized to maximize the N50. Assembled contigs for each strain were annotated with the National Center for Biotechnology Information Prokaryotic Genome Annotation Pipeline and deposited in GenBank (NCBI BioProject: PRJNA322208).

Population genomic analyses

We constructed a neighbor net genealogical network for 28 White Creek *F. thermalis* strains (including eight MLH3 strains) with SplitsTree version 4.14.4 (http://www.splitstree.org) for a concatenated alignment of 2,057,562 nucleotides from 2,011 polymorphic protein-coding genes. For each polymorphic protein-coding gene, genetic differentiation between MLH3 strains and other White Creek strains was estimated by Φ_{ST} (a measure of relative genetic differentiation between sub-populations based on nucleotide diversity, π), as in Sano et al. [37]. Genes exhibiting significantly high genetic differentiation between MLH3 and other strains were identified with a false discovery rate of 5% by the likelihood approach of Whitlock and Lotterhos [52], implemented in the OutFLANK R package (https://github.com/whitlock/OutFLANK). A Manhattan plot of the OutFLANK results was produced with the qqman R package, using the draft genome assembly (comprising 25 contigs ranging from ~2-600 kbp in length) for *F. thermalis* strain JSC-11 as a reference. For SNP loci that were completely differentiated between MLH3 and other strains, we next determined whether the MLH3 allele was ancestral or derived by comparison with aligned orthologous sequences from diverse *F. thermalis* strains from around the world. To assess whether any flanking non-coding variation was linked to a candidate gene, sliding windows of Φ_{ST} were estimated from π

estimates obtained for aligned genome contigs containing the candidate gene with DNASP version 5.10 [53]. A window length of 100 nt and a step size of 25 nt was used.

Acetylene reduction assays

N_2 fixation rates were determined by the acetylene reduction method [63]. For each strain, triplicate cultures were grown as above at 37°C and 55°C at a light intensity of 105 ± 5 μmol photons m^{-2} s^{-1} of cool white fluorescent light. Cultures of growing cells were homogenized with a tissue grinder and then assayed for four hours in the dark at the respective growth temperatures in 20 mL crimp-sealed vials containing 10 mL of fresh medium and 5 mL of acetylene gas (produced by the addition of 5 g of calcium carbide to 100 mL of deionized water). Blank-corrected ethylene production was measured using flame-ionization detection gas chromatography with a Shimadzu GC-2014 (Shimadzu, Kyoto, Japan). To estimate the light dependent component of N_2 fixation ($N_{total} - N_{dark}$), these data were compared with data obtained in the light that had been simultaneously acquired and were reported in Hutchins and Miller [64].

F. thermalis growth with nitrate

Growth rates in the presence of nitrate were determined at 55°C on a 12 h/12 h (light-dark) cycle and at a light intensity of 100 μmol photons m^{-2} s^{-1} of cool white fluorescent light for three strains each of White Creek *F. thermalis* with the MLH3 or MLH6 haplotype, respectively. For each strain, growing stock cultures were homogenized with a tissue grinder and transferred to fresh triplicated Erlenmeyer flasks containing 75 mL of D medium (which contains nitrates as a source of N) to a final optical density at 750 nm of 0.001. Growth was monitored with a Beckman Coulter DU 530 spectrophotometer by the change over time in culture optical density.

QUANTIFICATION AND STATISTICAL ANALYSIS

Genes exhibiting significantly high genetic differentiation between White Creek *F. thermalis* MLH3 strains and other strains were identified with a false discovery rate of 5% by the likelihood approach of Whitlock and Lotterhos [52], implemented in the OutFLANK R package (https://github.com/whitlock/OutFLANK). Growth and physiology data collected from the White Creek *F. thermalis* population were analyzed with linear models implemented with JMP version 10 (SAS Institute). For correlation analysis of physiological data collected from *Fischerella* strains related by a branching phylogeny, we used the Ornstein-Uhlenbeck phylogenetic generalized least-squares model implemented by COMPARE (http://www.indiana.edu/~martinsl/compare/v46b/compare). This approach relaxes the assumptions of standard least-squares analysis that are likely to be violated for comparative phenotypic data collected from organisms that are related to each other to different degrees, most notably the assumption of statistical independence. Details of the statistical analyses can be found in the Results and Discussion text.

DATA AND CODE AVAILABILITY

The genome data used in this study are available at NCBI BioProject: PRJNA322208. Heterocyst glycolipid composition data are included in Table S1 and Data S1.

Current Biology, Volume *30*

Supplemental Information

Cellular Innovation of the Cyanobacterial Heterocyst by the Adaptive Loss of Plasticity

Scott R. Miller, Reid Longley, Patrick R. Hutchins, and Thorsten Bauersachs

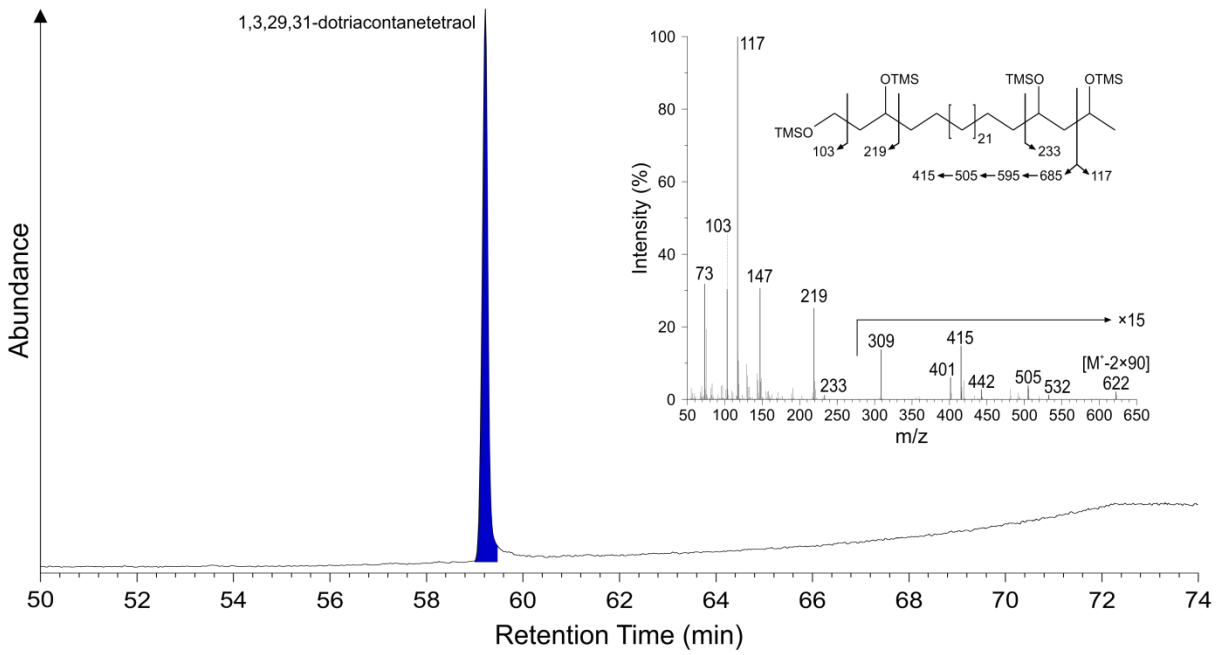

Figure S1. *Fischerella* HG_{32} triol structural isomers share the same aglycone moiety.

Related to Figure 1. Partial gas chromatogram showing the presence of 1,3,29,31-dotriacontanetetraol (i.e., the degradation product of HG_{32} triol) in the polar fraction of *Fischerella thermalis* WC 217 grown at 55 °C. Acid hydrolysis of the cell material resulted in the release of only one aglycone moiety indicating that the high diversity of intact HG molecules (with up to four structural isomers) observed in HPLC-MS^2 is due to differences in the nature and/or configuration of the sugar headgroup and not related to changes in the position and orientation of the functional groups attached to the carbon chain.

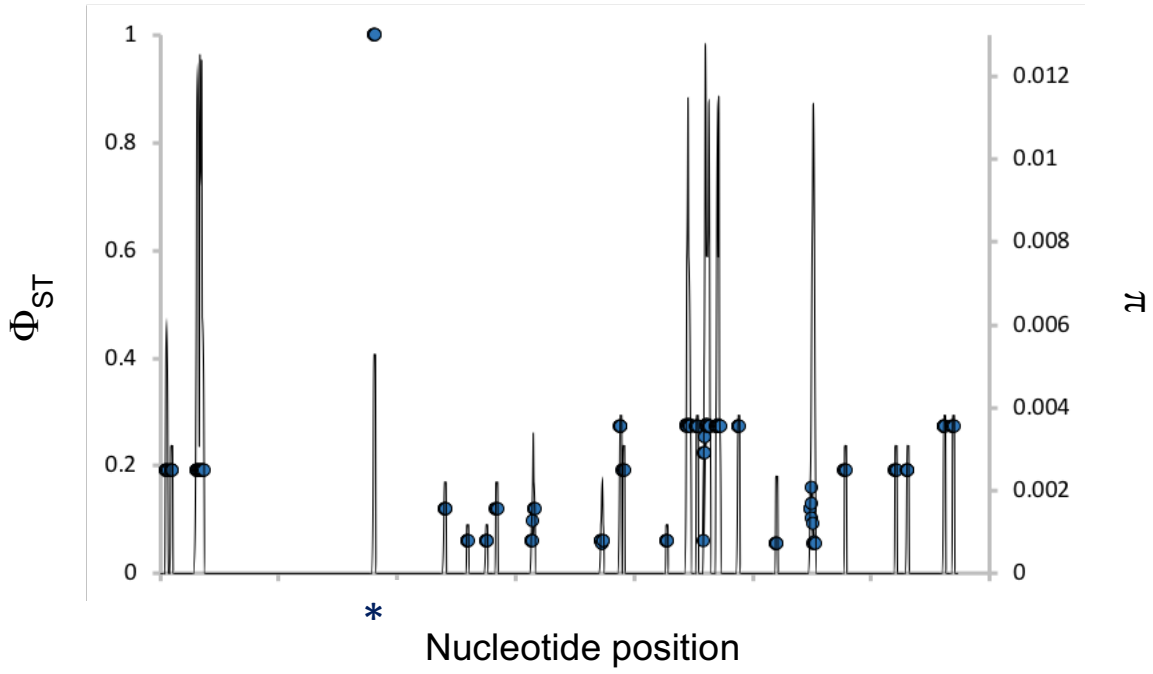

Figure S2. The *hglT* SNP is the only fixed genetic difference in the HGL expression island between high and low plasticity strains of White Creek *Fischerella thermalis*. Related to Figure 4. Sliding window of genetic variation (nucleotide diversity π, line) and genetic differentiation (Φ_{ST}, closed circles) between *F. thermalis* MLH3 strains and other White Creek strains for a ca. 34 kb region (axis ticks are 5 kbp increments) of the heterocyst glycolipid (HGL) gene expression island. The window length was 100 nt with a step size of 25 nt. Only the *hglT* candidate SNP (asterisk) is significantly differentiated between the two groups of strains (Φ_{ST} = 1).